The Rosat PSPC Spectrum of PKS2155-304

November 7, 1993

Abstract

The x-ray bright BL Lac object PKS2155-304 was observed with the ROSAT PSPC on two separate occasions: once on May 6,1991 and again on November 17, 1992. Fits to the extracted spectra from the two epochs revealed differences in the behavior of the source. There was a 45% drop in flux between the observations δf_x(0.2-2.0 keV)$\sim$ 1.1 ergs/cm^2/s, as well as differences in the spectra. The later observations were well fit with a simple power law; however, the earlier spectrum appears more complex, and requires an additional feature. We modelled this as an absorption notch or edge. Similar absorption by hot gas, apparently intrinsic to the source, has been detected with other instruments in this and other BL Lac objects. However, we believe the source of the feature in our earlier data is instrumental and is probably the result of a small temporal gain shift ($\sim 1-2\%$) in the response matrix.

Diane M. Gilmore
Science Data Analyst
Space Telescope Science Institute • Baltimore, Maryland

1 Introduction

Previous observations of the x-ray bright BL Lac object PKS2155-304 have detected an x-ray absorption feature at ~0.6 to 0.7 keV in spectra taken with the Objective Grating Spectrometer (OGS) aboard the *Einstein Observatory* (Canizares and Kruper, 1984), as well as in spectra from the Broad Band X-ray Telescope (BBXRT) in December 1990 at roughly the same energy (Madejski et al., 1992). The feature is thought to be due to Lyα absorption of O_{VIII} ($E_{rest} \sim 654eV$) at the redshift of the source, $z \sim 0.117$ (Bowyer at al., 1984).

In this poster, we present results from our Rosat PSPC observations of the source, the purpose of which was to attempt to detect and characterize the x-ray absorption feature discussed above. The PSPC-B detector was used to observe PKS2155-304 on two different occasions - May 6, 1991 and Nov 17, 1992.

2 Data Reduction

Background light curves were constructed from photons taken from annuli centered on the source and from 3.5 to 10 arcmin in radius. At 3.5 arcmin, the cnt/pix from the source is at ~.01% of the peak value. The background light curve of the May 1991 data has a period of very high background count rate during the final 350 seconds of GTI3, and brief periods of no counts during the first 35 seconds of GTI 1 and 2. These periods were filtered out before extracting spectra. The background light curve of the November 1992 data appears normal, with no troubling periods of either very high or low background count rate. No time filtering was performed on this data set.

The last two exposures of the May 1991 data are separated by 3.5 days from the first GTI of that epoch, and by 3 seconds from each other. Time-clipping the last GTI left it with just 268 seconds (compared to the first GTI which had 752 seconds) and correspondingly large errors on its spectral parameters.

In addition to extracting spectra of the summed Good Time Intervals, spectra from each of the corrected GTI intervals of the two epochs were extracted (time-filtered) into separate data files for further analysis. To define source regions, source centers were obtained by centroiding on a block-factor 4 image near the peak emission seen in channels 18 through 201 (0.18 to 2.0 keV). Lower energy channles were excluded to avoid the "ghost image" problem (caused by scattering off the fine wire mesh) which has been shown to occur in pi channels lower than about 15 (0.15 keV) (Hasinger et al., 1992). The ROSAT centroid positions are RA 21:58:52, DEC -30:13:38 (2000) for the first epoch, and RA 21:58:52, DEC -30:13:25 (2000) for the second epoch. The precise optical (GASP) position is RA 21:58:52, DEC -30:13:32.7 (2000). We believe the discrepancies can be attributed to the error in Rosat pointing which has been shown to be as much as 10 arcsec (ROSAT Status Report No. 29).

Photons from all 256 energy bins were collected from a source region defined as a circle centered on the source, with a radius of 2 arcmin, and were later filtered by energy (see below). This radius includes 99% of all photons from all

energies between 0.2 and 1.7 keV (see Figure 7, Hasinger et al., 1992). Background regions were taken to be annuli from the same file centered on the source, with radii from 3.5 to 10 arcminutes (see Figure 1).

No vignetting correction was necessary because the source was an on-axis point source, and because thecount rate measured over the background annulus was so low (~0.5 cts/sec). The effect of vignetting at 10 arcmin, the largest background radius, is about 5%, judging from the exposure map at 1 keV provided by SASS. Since the source is so bright (~35 cts/sec) relative to the background, vignetting should have a minimal affect on the spectral analysis.

3 Spatial Analysis

When fit with a two-dimensional Gaussian, using PI channels 18 through 201 (0.18 to 2.01 keV), the source showed a FWHM of about 33 to 34 arcsec in both datasets. The lower energy limit (0.18 keV) was chosen to avoid the ghosting effect, and the upper limit corresponds to 2 keV above which the PSF is not known. A fixed-energy model image generated at the weighted mean energy (0.63 keV) of a power law fit to the source (with spectral index 2.4) yielded a FWHM ($\sim$ 30 arcsec) less than that of the data.

We computed radial profiles for our data in three narrow energy bands (soft: 0.18 to 0.3 keV, medium: 0.4 to 0.7 keV, and hard: 1.0 to 2.0 keV) for comparison with model profiles. The models were generated at the mean, or spectrum-weighted, energy for each band. The data profiles matched the model profiles very closely indicating that the discrepency seen between the wide band images is due to blending of the different PRFs in the data.

The source, displayed with all energy channels included, was slightly asymmetric for each epoch. The images appeared more symmetric and smaller at harder energies, indicating that "ghosting" was occurring at the lower energies (scattering of low-energy photons off the fine wire mesh). Taking photons from small regions in detector coordinates, new images of the source were made. The sources appeared asymmetric, with tails pointing in a direction parallel to the wobble. However, subsequent filtering of the low energy channels (1-17) showed that the aspect errors were caused primarily by these low-energy photons, the ones most likely to have been scattered by the wire mesh. The Nov 92 data shows residual asymmetries, even after removing the low energy photons. We conclude that there are larger aspect problems for the latter dataset. The small aspect solution errors should have no effect on the spectral analysis since a large source aperture (2 arcmin) was used when extracting spectra, and only channels above 0.14 keV were considered in the spectral fits.

4 Spectral Analysis

The count rates for each of the time-clipped Good Time Intervals are listed below in Table I for both epochs of data. Note that the count rate of the later epoch has dropped by 45% of that of the earlier epoch, which cannot entirely be the effect of a gain shift (Rosat Status Report No. 64).

May 1991 data (channels 4 through 30, energies .14 to 2.02 keV)
GTI 1 (752 seconds): 35.46 $\pm$ 0.22
GTI 2 (798 seconds): 33.94 $\pm$ 0.21
GTI 3 (268 seconds): 33.88 $\pm$ 0.36
SUMMED (1818 seconds): 34.56 $\pm$ 0.14

Nov 1992 data (channels 4 through 30, energies .14 to 2.02 keV)
GTI 1 (263 seconds): 19.73 ± 0.27
GTI 2 (812 seconds): 18.77 ± 0.15
SUMMED (1075 seconds): 19.01 ± 0.13

Table I. Count rates for the Good Time Intervals of each of the 2 epochs.

Using the standard MPE SASS binning, thirty-four channel spectra were extracted in IRAF/PROS, and were analyzed using the x-ray spectral fitting package XSPEC version 8.2 (Shafer et al., 1991). During spectral analysis, channels from 1 to 3 were ignored because of various soft-energy contaminants in the spectrum (due to the limb of the bright earth, etc.), and channels 31 to 34 were also ignored, since the gain at the highest energies (above 2.0 keV) is less well known (Rosat Status Report No. 54). Over the range of channels used in our fits, the final summed spectra have more than 50 cts/bin, and the individual GTI spectra have more than 18 cts/bin in every case, so that the chisquare statistical method of analysis is applicable (Cash, 1979).

In order to compensate for the residual gain shift in spectra taken after the switch from high to low gain state in the detector which occured on Oct 14, 1991 (Rosat Status Report No. 64), we used two different response matrices to analyze data from the two epochs. Spectral fits for the earlier data set were made using the response matrix from early March 1991, pspcb_92mar11.rsp, while spectra from the latter data set were analyzed with a matrix from January 1993, pspcb_93jan12.rsp.

To avoid overinterpretation of spectral features, we added (in quadrature) a 2% systematic error to the errors of each of the spectra of the individual exposures, and to the summed spectra as suggested in the PSPC Calibration Guide (1993, Turner, J. and George, I.).

Many types of fits were tried including a simple power law, broken power law, and double power law. Each was tried with and without an absorption feature (notch or edge), and all included a low-energy cutoff (N_H) due to galactic absorption.

5 Results of Spectral Fitting

First Epoch Results:

A power law cutoff at low energies with free local column density produced acceptable fits for the summed spectra of both epochs. When fit individually however, the second exposure of the first epoch was not well fit with a simple power law ($\chi^2_{DOF} = 1.34$ for 24 dof), but appears more complex. The second exposure is separated by ~3.5 days from the first and has 798 seconds, compared to 752 seconds in the first exposure of this epoch. This exposure required an

added component to the power law model. We tried modelling the new component as a second power law (in the form of a broken power law fit), and also as an absorption feature (a notch or an edge) added to the simple power law model. All three models produced acceptable fits for each of the individual GTIs and the summed spectrum; however, a notch improved the fits significantly (at a significance of $\gg$99% for an added notch, >99% for an added edge, and >99% for a second power law (with break energy fixed at 1.0 keV).

The spectral parameters for the different fits are shown in Table II. Fits and residuals for the simple power law, power law plus notch (covering fraction fixed at $C = 1.0$, and power law plus edge fits, are shown in Figure 2.

For the added edge fits, the edge appears at an energy of about 0.28 keV (with a poorly determined optical depth, τ_{max}), at the location of the carbon edge. The carbon edge is known to have been fit poorly in the early response matrix (Rosat Status Report No. 64), however, this is currently the best available matrix for use with data taken before the gain switch of October 14, 1991.

Freezing the column density at the Galactic value of 1.36×10^{20}atoms/cm^2 (Lockman and Savage, recently measured), we again tested the significance of the added notch. The F-test still showed that the notch was significant (at a confidence level >99% for the summed data), though again, GTI2 was the most improved exposure. The simple power law fits give a photon index of ~2.4, which doesn't change significantly when the notch is added. The notch occurs at an energy of ~0.43 keV, with a poorly-determined width of about 60eV (notch parameters correspond to the fit of GTI2, with N_H fixed at the Galactic value). For comparison, the spectral resolution of the detector at 0.4 keV is about 260 eV.

Double power law models did not improve the fit to the data. A broken power law (with break energy held fixed at 1.0 keV) gave somewhat better chisquare values than a simple power law (the second power law was significant at roughly the 99% level), however adding a notch significantly improved the fits again at the >99% level. A broken power law plus notch fit (E_{break} fixed at 1.0 keV) to the summed spectrum preferred a notch at 0.48 keV, too low to correspond to the Oxygen absorption feature found in the OGS and BBXRT spectra of the source. The mild spectral steepening of $\delta\Gamma = 0.1$ was not significant. The broken power law did not improve the fits to the other GTIs of this epoch. In fact, none of the added features we tried improved fits to the spectra of the other GTI significantly with respect to a simple power law.

*** insert table 2, followed by Fig. 2.

Second Epoch Results:

The November 1992 data yielded very good fits (χ^2_{DOF} <1.0) with a simple cutoff power law of photon index Γ ~2.6 and neutral column density $N_H \sim 1.48 \times 10^{20}$ atoms/cm^2.

Adding a notch did not improve the fits to these data significantly. Holding the column density fixed at the Galactic value and adding an edge to the power law did, however, improve the fits (at a confidence level of ~97%), though the edge energy was placed at E_{edge} ~1.1 keV, with a maximum absorption depth of only τ_{max} ~0.2. When the column density was allowed to vary, no significant improvement to the fits were obtained beyond those of the simple power law model.

The broken power law model improved the fits significantly only when the column density was held fixed at the Galactic value. The summed spectra improved at a confidence level of ~97%, and gave a break energy of E_{break} ~0.7 keV, with photon indices of ~2.5 and ~2.7, for the low and high energy power laws, respectively. There doesn't appear to be any feature at roughly 0.4 keV as in the first epoch data, or at a higher energy, for that matter.

The best fit power law, power law plus edge, and broken power law fits and residuals are plotted in Figure 3. Table III contains the best fit parameters found for the second epoch spectra.

It is interesting to note that the column density and photon index have increased since the last epoch, for simple power law fits to the spectra. The spectral differences are significant, as demonstrated by the disjoint chi-square contours plotted in Figure 4 for a power law fit to the summed spectra of both epochs. The spectrum has steepened (softened) by $\delta\Gamma \sim 0.2$ and N_H has risen by about 10%, while the flux has dropped by ~45%. This correlation bewteen spectral hardness and source intensity has been seen in this and other BL Lac objects.

***insert table 4 ***

6 Timing Analysis

The Kolmogorov-Smirnov (KS) test was used to detect variability in the integrated light curve of PKS2155-304. We have plotted the KS test for each of the epochs in Figure 5. The residuals with respect to a constant count rate integrated over time are shown in the bottom panels of Figures 5a and 5b. The effect of the telescope wobble can be clearly seen as a periodic variation in the residuals, with a period of about 100 seconds (the wobble is actually a 400-second period, but light is scattered from the source each time it passes under a wire of the wire mesh support structure; this appears to happen about once every 100 or so seconds). We are more interested in the largest deviation averaged over the wobble time. The deviation appears to be about 0.01 for the May 1991 data, which indicates variability with >99% significance over the period of the observation (~3.5 days). The second epoch also apparently shows variability with >99% significance by the KS test over a period of ~1.5 hrs.

The absorbed flux densities (in Tables II and III) for the best power law fits to the summed spectra indicate a decrease in flux by 45% by the source over the one and a half years between the observations.

7 Discussion

MPE has studied the sytematic errors in the old response matrix (pspcb_92mar11) seen in high signal-to-noise PSPC data and find a) a deficiency of measured counts in the trough above the carbon edge at 0.4 keV, with associated excesses at 0.2-0.3 keV and 0.6 to 0.98 keV, b) an excess of measured counts above 2 keV (MPE Status Report No. 10, 1992, reissued as Rosat Status Report No. 29). The magnitude of these errors, for data taken after the gain switch in October 1991, is about 1 sigma per channel. The residuals to a power law fit to our earlier data set for PKS2155 show a deficiency of measured counts at about 0.4-0.5 keV, where an absorption feature would fit, and an excess of counts from about 0.7-1.0 keV, behavior similar to the residual systematic errors which occur in fits of newer data (taken after the gain switch of October 14, 1991) using the old matrix.

Even though we are using the early matrix (pspcb_92mar11) which best represents data taken before the gain switch, we suspect that there is an additional residual gain shift which is causing the feature we fit as a trough in our earlier data. Brinkmann (1993, in prep.) has found that a change in gain as small as $\sim$ 1% can cause noticable changes in the spectral fit at or near the carbon edge, for steep (Γ $\sim$2.7) spectral sources like PKS2155. This is especially a problem for our source because of its high count rate. If we compare the notch depth at 0.4 keV to the height of the power law spectrum there, we see a deficiency in measured counts of $\sim$ 14%, comparable to the size of the drop ($\sim$ 11%) in expected counts seen in the 1992 spectrum of MRK421, used as a calibration source for the PSPC, when fit with the old (pspcb_92mar11) matrix (Turner J. and George, I., 1993).

In summary, even though the notch fits are significant for the second exposure of the May data, a notch in the first exposure of the first epoch cannot be ruled out. If this is the case, it is likely that we are seeing detector response errors rather than a physical feature in the source spectrum. Given that the edge fits place the edge at an energy of 0.28 keV, at just the location of the carbon edge, and that the shape and size of the feature is similar to the feature found in the residuals of the best fit to the MRK421 data, it is likely that we have detected response matrix error in our early (A0) data. We find no other spectral features in our PSPC data for either epoch.

Brinkmann et al. (1993, in prep.) has studied PSPC data for the same source taken in November 1991 as part of a multi-frequency campaign. The source was found to be exceptionally bright ($\sim$50cts/s), but dropped by roughly 30% over the four days of the observations, with no attendant change in spectral parameters. His data are well fit by a simple power law of photon index Γ $\sim$2.7, with Galactic absorption; he finds no evidence of a spectral feature in the energy range 0.6-0.7 keV.

The presence of a higher energy line cannot be ruled out, however given the problems with temporal gain variations in the PSPC, detection of such an x-ray feature as the one found in OGS and BBXRT data becomes difficult.

8 References

Bevington, P. 1969, "Data Reduction and Error Analysis for the Physical Sciences".
Bowyer, S. et al. 1984, ApJ Letters, 278, L103.
Brinkmann, W. et al., 1993, in prep.
Canizares, C., and Kruper, J. 1984, ApJ Letters 278, L99.
Cash, 1979, Ap.J. 228, 939.
Hasinger, et al., 1992, Legacy No. 2.
Lampton, M., Margon, B., Bowyer, S., 1976, Ap.J. 208, 177.
Lockman and Savage, in prep.
Madejski, G., et al. 1991, in "Frontiers in Xray Astronomy", eds. Y. Tanaka and K. Koyama, Univ. Academy Press, Tokyo, p.583
Seward, F., and Wilkes, B. 1991, ROSAT-PROS Users Guide, V. 1.1
Shafer, R., Haberl, F., Arnaud, K., and Tennant, A. 1991, Xspec User's Guide, version 2, ESA TM-09.
Turner, Rosat Status Reports No. 29, 54, and 64.
Turner, T.J. and George, I. M., ed. 1993, Rosat PSPC Calibration Guide (Draft).

Fits to the First Epoch Spectra (May 1991)

		χ^2	N_H (exp20)	Γ_1	Normalization (exp-2)	Flux[v] (exp-10)
power law[s]	sum	0.64	1.31(1.19-1.43)	2.38(2.33-2.44)	6.46(6.34-6.59)	2.37
power law[r]	sum	0.65	1.36 (frozen)	2.41(2.39-2.42)	6.47(6.38-6.56)	2.38
power law[s]	gti2	1.34	1.34(1.19-1.50)	2.38(2.31-2.45)	6.46(6.30-6.62)	2.35
power law[r]	gti2	1.28	1.36 (frozen)	2.39(2.37-2.40)	6.46(6.34-6.58)	2.36

		χ^2	N_H (exp20)	Γ_1	Normalization (exp-2)	E_{line} keV	E_{width} keV	Flux[v] (exp-10)
p.l.+notch[u]	sum	0.35	1.46(1.24-1.70)	2.45(2.36-2.55)	6.55(6.37-6.75)	0.45(0.00-0.65)	0.05(0.00-0.20)	2.29
p.l.+notch[t]	sum	0.40	1.36 (frozen)	2.41(2.39-2.43)	6.51(6.37-6.66)	0.44(0.26-0.63)	0.04[f]	2.29
p.l.+notch[u]	gti2	0.69	1.67(1.38-2.05)	2.54(2.39-2.71)	6.64(6.40-6.92)	0.38(0.36-0.54)	0.20[f]	2.05
p.l.+notch[t]	gti2	1.00	1.36 (frozen)	2.39(2.36-2.43)	6.53(6.33-6.73)	0.43(0.32-0.57)	0.06[f]	2.19

		χ^2	N_H (exp20)	Γ_1	Normalization (exp-2)	E_{edge} keV	τ_{max}	Flux[v] (exp-10)
p.l.+edge[u]	sum	0.41	1.62[f]	2.53(2.35-2.72)	6.78[f]	0.28[f]	1.08(0.00-2.52)	2.20
p.l.+edge[t]	sum	0.54	1.36 (frozen)	2.42(2.38-2.47)	6.55(6.37-6.73)	0.27[f]	0.29(0.00-0.70)	2.32
p.l.+edge[u]	gti2	0.78	2.04(1.47-2.70)	2.71(2.45-2.99)	7.16(6.57-7.87)	0.27(0.26-0.28)	2.37(0.51-4.69)	2.07
p.l.+edge[t]	gti2	1.24	1.36 (frozen)	2.41(2.36-2.49)	6.54(6.32-6.78)	0.27[f]	0.30(0.00-0.85)	2.30

		χ^2	N_H (exp20)	Γ_1	E_{break} keV	Γ_2	Normalization (exp-2)	Flux[v] (exp-10)
broken p.l.[t]	sum	0.49	1.20(1.03-1.39)	2.32(2.22-2.42)	1.0 (frozen)	2.50(2.34-2.67)	6.62(6.37-6.87)	2.35
broken p.l.[t]	sum	0.68	1.36 (frozen)	2.40[f]	1.1[f]	2.47[f]	6.51[f]	2.38
broken p.l.[t]	gti2	0.97	1.15(0.90-1.38)	2.25(2.13-2.38)	1.0 (frozen)	2.64(2.41-2.88)	6.80(6.46-7.13)	2.31
broken p.l.[t]	gti2	1.20	1.36 (frozen)	2.36(2.32-2.40)	1.0(0.0-40.0)	2.58[f]	6.64[f]	2.36

		χ^2	N_H (exp20)	Γ_1	E_{break} keV	Γ_2	Normalization (exp-2)	E_{line} keV	E_{width} keV	Flux[v] (exp-10)
b.p.l.+notch[t]	sum	0.32	1.38(1.05-1.79)	2.40(2.23-2.69)	1.0 (frozen)	2.50(2.30-2.72)	6.63(6.31-6.97)	0.47[f]	0.03(0.00-0.20)	2.32
b.p.l.+notch[s]	sum	0.31	1.36 (frozen)	2.40(2.36-2.44)	1.0 (frozen)	2.51(2.33-2.69)	6.63(6.36-6.93)	0.47(0.27-0.67)	0.03(0.00-0.19)	2.32
b.p.l.+notch[t]	gti2	0.61	1.45(1.03-2.25)	2.40(2.18-2.84)	1.0 (frozen)	2.65(2.35-2.96)	6.83(6.37-7.29)	0.47(0.35-0.65)	0.06[f]	2.26
b.p.l.+notch[s]	gti2	0.60	1.36 (frozen)	2.35(2.31-2.40)	1.0 (frozen)	2.67(2.42-2.94)	6.86(6.49-7.26)	0.48(0.35-0.60)	0.05(0.01-0.21)	2.27

Key:
f = unconstrained
r = 90% error for 1 interesting parameter
s = 90% error for 2 interesting parameters
t = 90% error for 3 interesting parameters
u = 90% error for 4 interesting parameters
v = Absorbed flux in $ergs/cm^2/sec$

Table III. Spectral fits to the May 1991 sopectra using pi bins 4 through 30 (energies 0.14 through 2.02 keV).

Fits to the Second Epoch Spectra (November 1992)

		χ^2	N_H (exp20)	Γ_1	Normalization (exp-2)	Flux[v] (exp-10)		
power law[s]	sum	0.73	1.48(1.30-1.67)	2.57(2.49-2.66)	3.21(3.12-3.31)	1.27		
power law[r]	sum	0.77	1.36 (frozen)	2.52(2.50-2.54)	3.20(3.13-3.28)	1.25		
		χ^2	N_H (exp20)	Γ_1	Normalization (exp-2)	E_{edge} keV	τ_{max}	Flux[v] (exp-10)
p.l.+edge[u]	sum	0.62	1.34(1.05-1.66)	2.48(2.31-2.65)	3.36(3.12-3.64)	1.11(0.70-100.)	0.22(0-0.56)	1.26
p.l.+edge[t]	sum	0.60	1.36 (frozen)	2.49(2.44-2.54)	3.35(3.16-3.58)	1.11[f]	0.21(0-0.44)	1.26
		χ^2	N_H (exp20)	Γ_1	E_{break} keV	Γ_2	Normalization (exp-2)	Flux[v] (exp-10)
broken p.l.[t]	sum	0.62	1.36 (frozen)	2.48[f]	0.73[f]	2.65[f]	3.40[f]	1.26

Key:
f = unconstrained
r = 90% error for 1 interesting parameter
s = 90% error for 2 interesting parameters
t = 90% error for 3 interesting parameters
u = 90% error for 4 interesting parameters
v = Absorbed flux

Table IV. Fits for the November 1992 data using binned pi channels 4-30 (energies 0.14 – 2.02 keV).

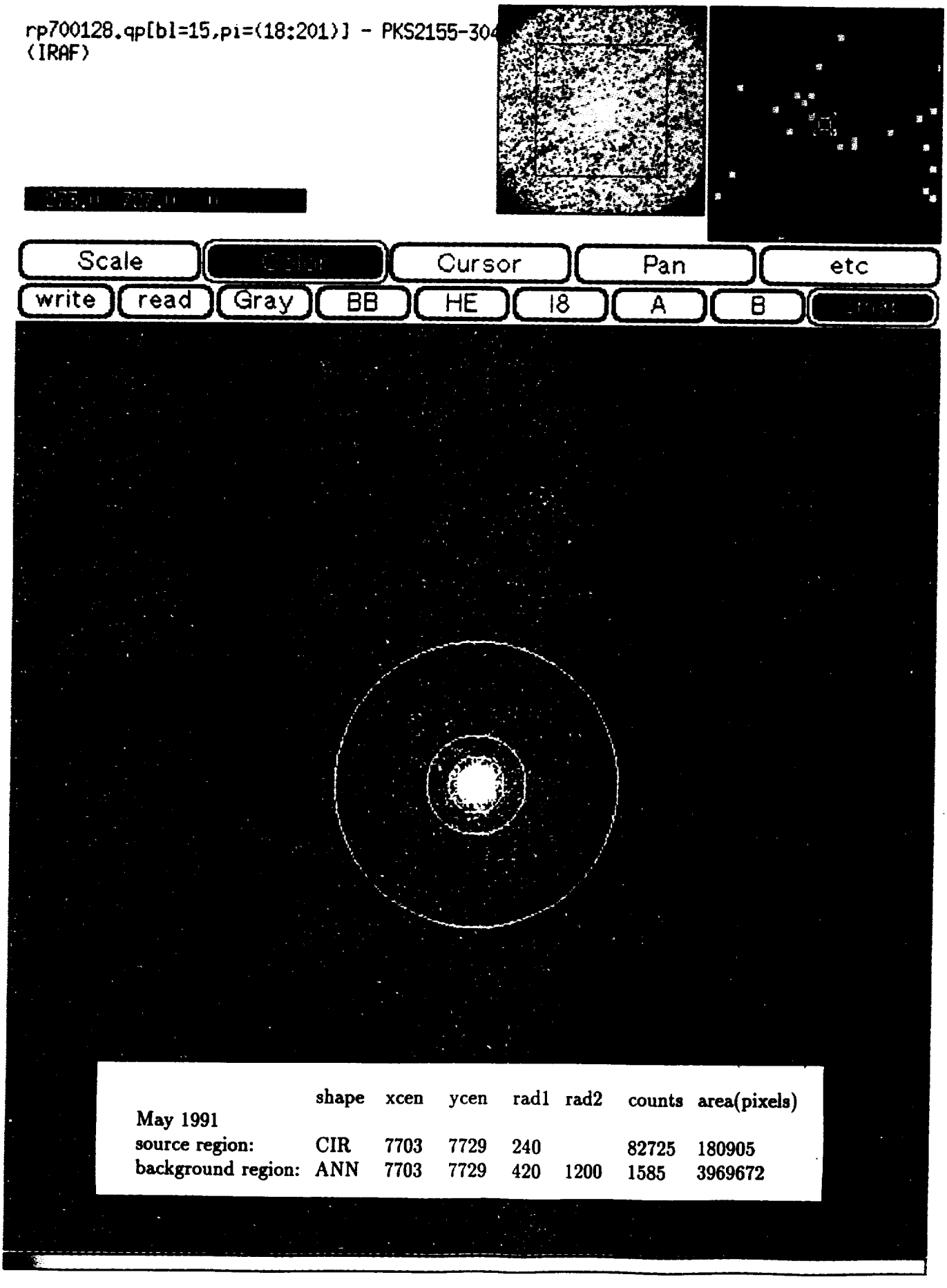

Figure 1. ROSAT PSPC-B image of PKS2155-304 (all photons included). On it are

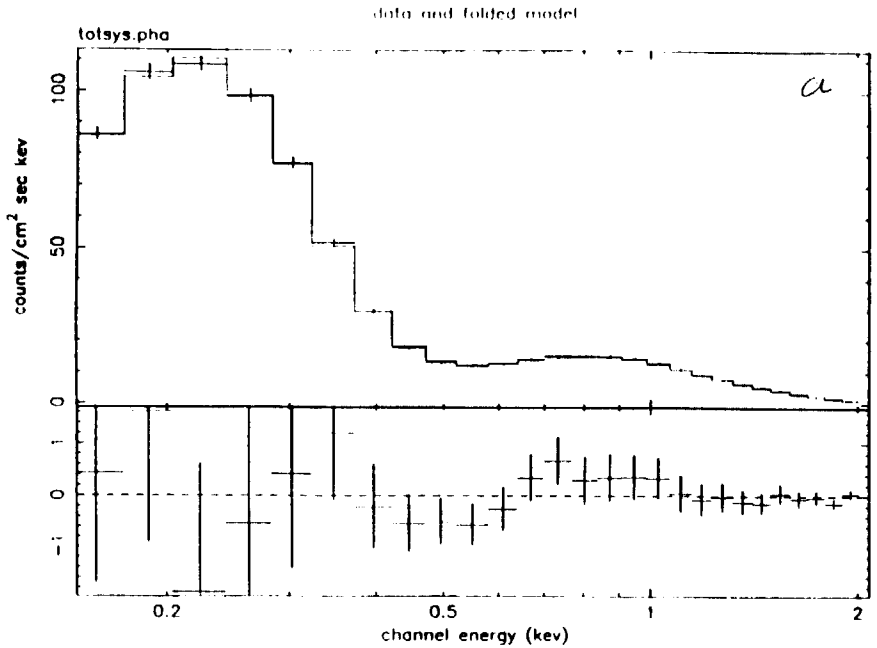

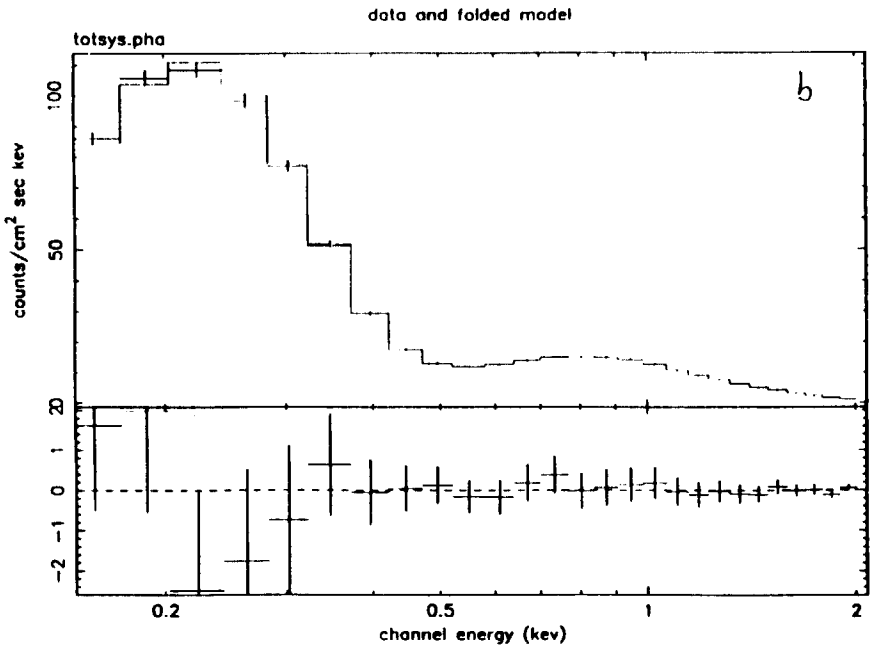

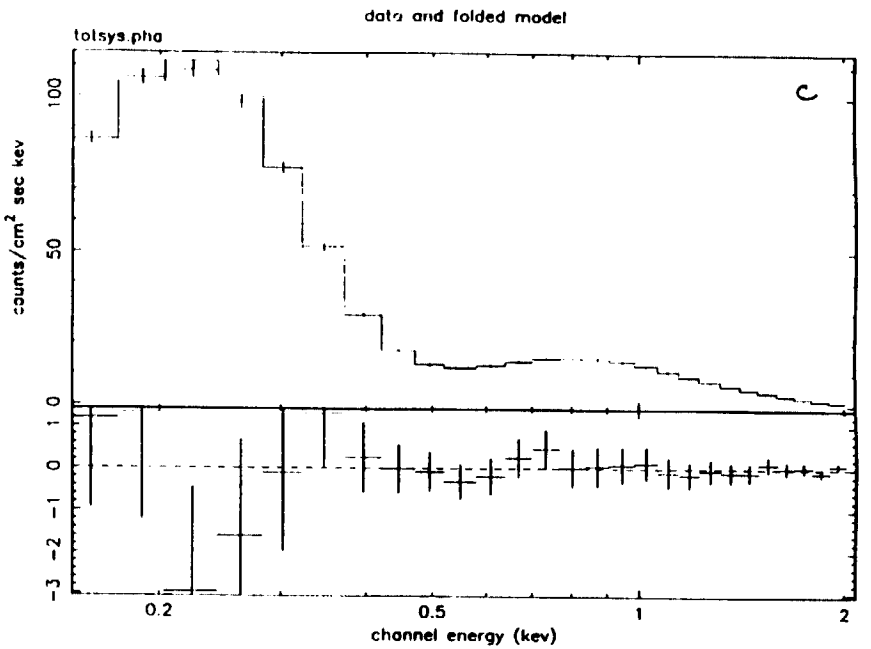

Figure 2. The fits and residuals to the fits of a) a simple power law model, b) a power law plus notch model, and c) a power law plus edge model for the May 1991 summed spectrum. The error bars include a 2% added systematic error.

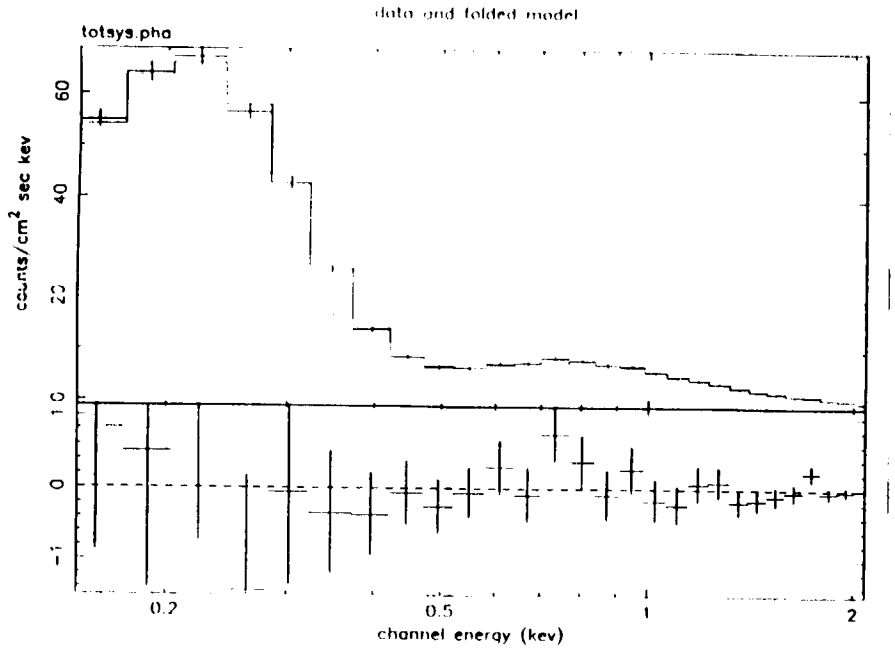

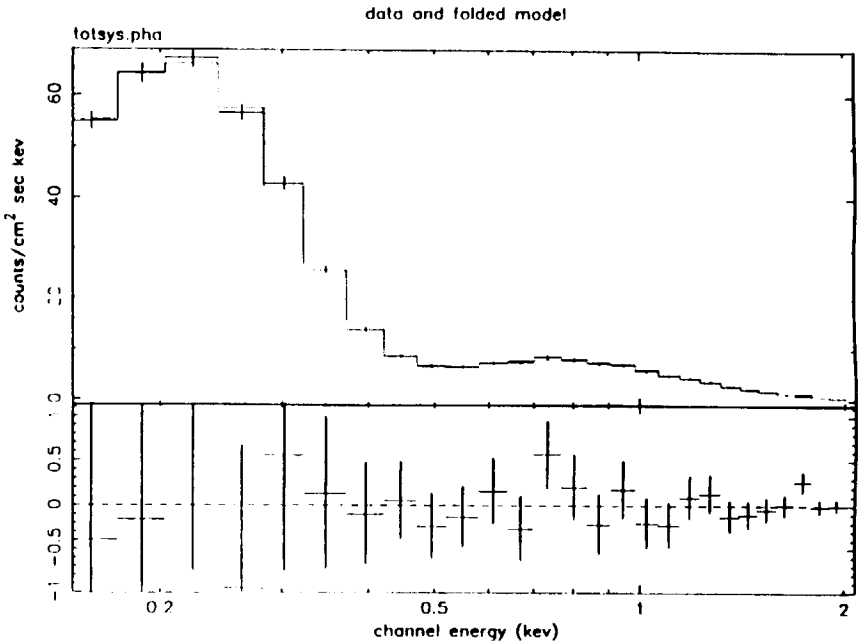

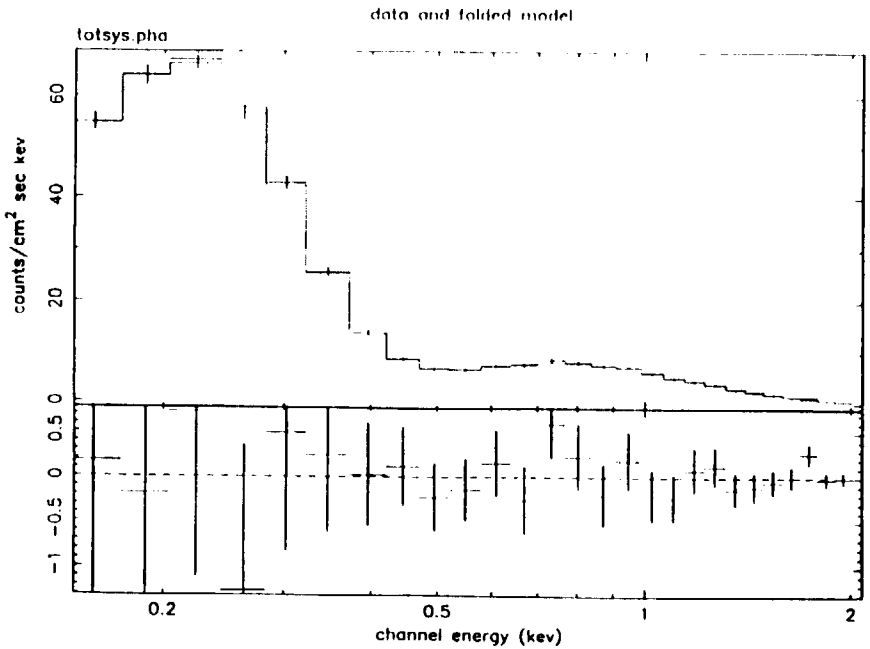

Figure 3. The fits and residuals to the fits of a) a simple power law model, b) a power law plus edge model, and c) a broken power law model ($N_H = 1.36 \times 10^{20}$, held fixed) for the summed spectra of the Novbember 1992 data. The error bars include a 2% added systematic error.

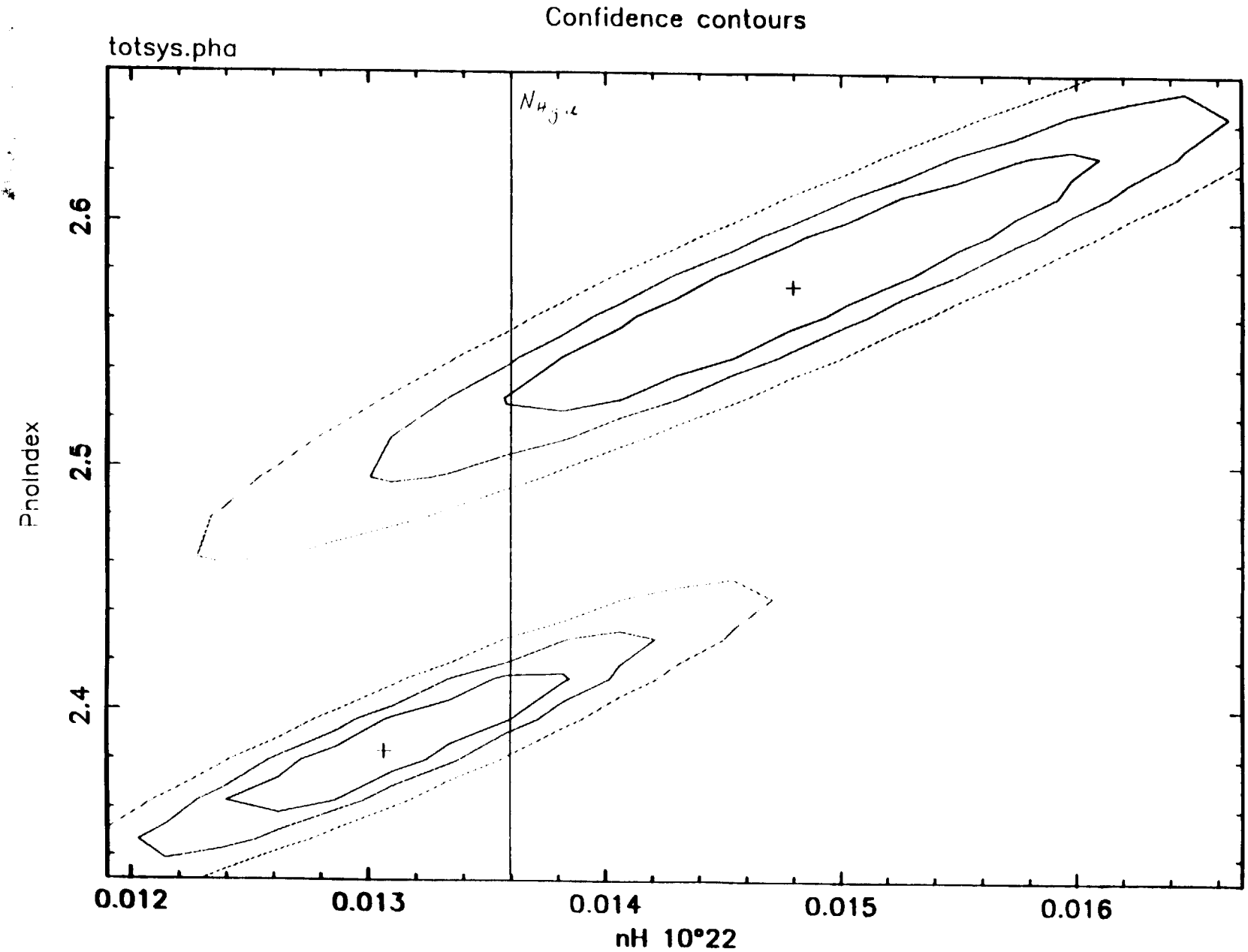

Figure 4. Chisquare contour levels of 68%, 90%, and 99% significance (for two interesting parameters) over parameters N_H and Γ from the best power law fits to the summed spectra of the two epochs. The contours at the lower left are from the May 1991 observation, when the source was brighter.

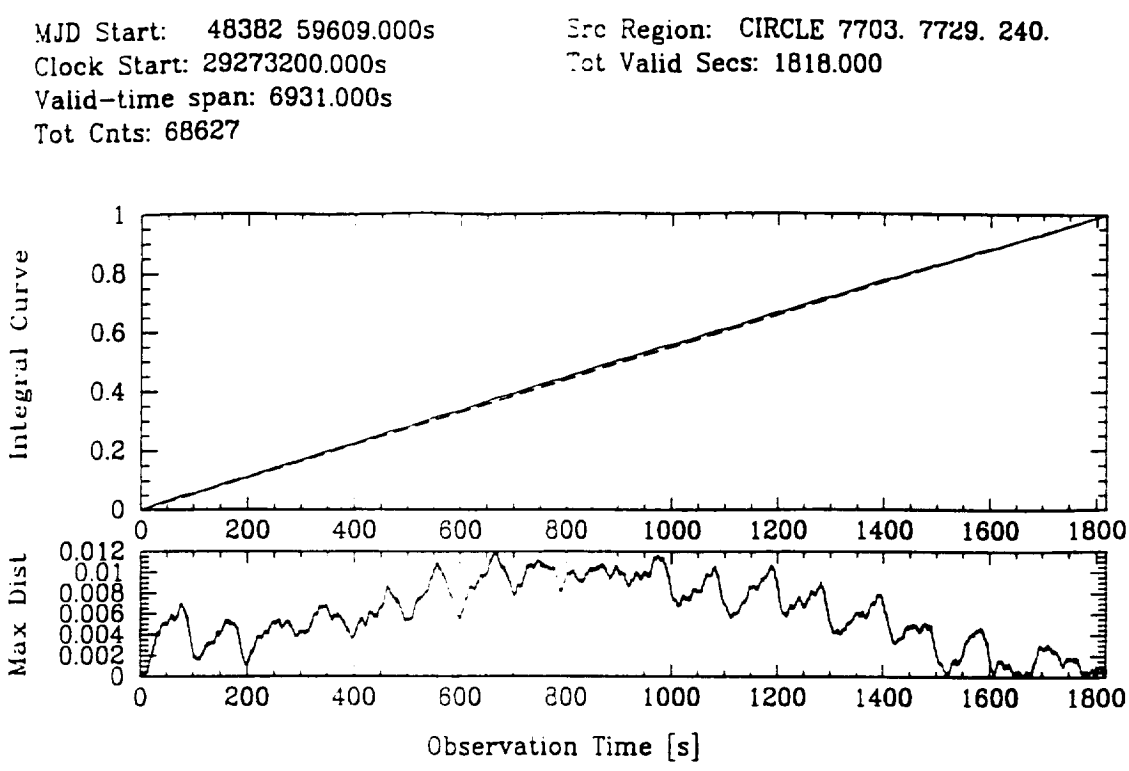

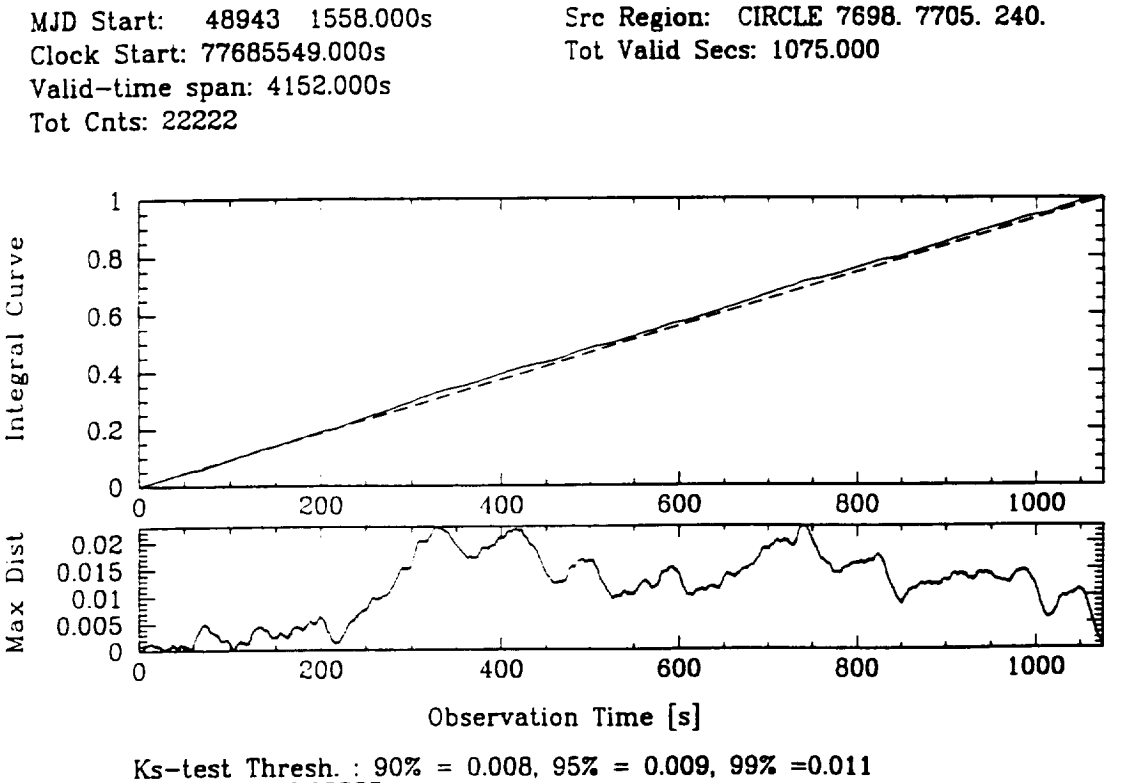

Figure 5. The KS-Test for each epoch showing short-term variability in the source integarted light curve compared to that of a source with constant count rate. 5a) The May 1991 observation; 5b) the Nov 1992 observation.

8 References

Bevington, P. 1969, "Data Reduction and Error Analysis for the Physical Sciences".
Bowyer, S. et al. 1984, ApJ Letters, 278, L103.
Brinkmann, W. et al., 1993, in prep.
Canizares, C., and Kruper, J. 1984, ApJ Letters 278, L99.
Cash, 1979, Ap.J. 228, 939.
Hasinger, et al., 1992, Legacy No. 2.
Lampton, M., Margon, B., Bowyer, S., 1976, Ap.J. 208, 177.
Lockman and Savage, in prep.
Madejski, G., et al. 1991, in "Frontiers in Xray Astronomy", eds. Y. Tanaka and K. Koyama, Univ. Academy Press, Tokyo, p.583
Seward, F., and Wilkes, B. 1991, ROSAT-PROS Users Guide, V. 1.1
Shafer, R., Haberl, F., Arnaud, K., and Tennant, A. 1991, Xspec User's Guide, version 2, ESA TM-09.
Turner, Rosat Status Reports No. 29, 54, and 64.
Turner, T.J. and George, I. M., ed. 1993, Rosat PSPC Calibration Guide (Draft).